All-electron first-principles calculations of clean surface properties of low-Miller-index Al surfaces

Juarez L. F. Da Silva*
Institut für Festkörperforschung, Forschungszentrum Jülich, D-52425 Jülich, Germany
(Received 23 September 2004; revised manuscript received 21 December 2004; published 25 May 2005)

We report a systematic theoretical study of the clean surface properties of the Al(111), Al(100), and Al(110) surfaces as function of the film thickness employing slabs with thicknesses up to 32 Å. Our calculations are based on density functional theory employing the all-electron full-potential linearized augmented plane-wave (FLAPW) method. Our results show clearly a periodic oscillatory behavior of the surface energies, work functions, interlayer relaxations, total density of states at the Fermi level as function of the slab thickness, however, similar behavior is not found for the occupied bandwidth at the Γ point. The magnitude of the oscillations decrease with an increase of the number of layers in the slab, as expected. We found that the period of the oscillations are almost the same for Al(111) and Al(110), however, the work functions and interlayer relaxations obtained for Al(100) show oscillations with a larger period (almost by a factor of two) compared to the Al(111) and Al(110) surfaces, which are explained in terms of the deep penetration of the surface states into the bulk region of the Al(100) surface. This new physical result, as well as the agreement between our FLAPW calculations and the available experimental results, are discussed in this paper.

DOI: 10.1103/PhysRevB.71.195416 PACS number(s): 68.47.De, 82.45.Jn, 71.15.Ap

I. INTRODUCTION

Three decades ago, Schulte[1] reported that electron densities, potentials, and work functions of thin jellium films calculated as a function of the film thickness show oscillations with a period of one-half the Fermi wavelength, which was attributed to quantum-size effects (QSE). For example, in ultrathin finite films electrons can move quasifreely in the directions parallel to the film surface, (x,y), while their motion perpendicular to the film surface, z, are quantized in a particle-in-a-box fashion due the presence of the vacuum.[2]

Through continuing evolution of the ultrathin metallic film technology, the theoretical predictions of QSE have been experimentally verified by studying the electrons near the Fermi energy by different techniques. For example, photoemission,[3] inverse photoemission,[4] electrical resistivity,[5,6] Hall effect,[7] scanning tunneling microscopy,[8] and low-energy electron microscopy.[9] Nowadays, first-principles calculations[10–18] have shown that the surface energy, work function, interlayer relaxations, and etc., of solid surfaces exhibit oscillations as function of the film thickness.

In theoretical calculations for periodic systems, a semi-infinite film is modeled using slabs with a finite number of layers. Hence, for many systems, QSE plays an important role in obtaining reliable (converged as function of the number of layers) surface properties, which are compared to experiments done on semi-infinite samples. Therefore, it is essential to know and understand the size and extent of QSE in the surface properties of thin films. Theoretically, the low-Miller-index Al surfaces are one of the most studied systems to better understand the size and extent of QSE.[10–14] Furthermore, calculations have also been done for lithium surfaces,[18] for Pb(111),[15,17] for Cu(111),[16] and other transition-metal surfaces.[10]

In spite of the large number of studies for low-Miller-index Al surfaces, the agreement between the calculations themselves, as well as with experimental results is far from satisfactory. For example, local-density approximation (LDA) surface energies are in the range 0.39–0.48 eV per surface atom for Al(111),[19,20] and $0.77-0.92$ eV per surface atom for Al(110).[19–21] Reported LDA work functions are in the range 3.70–4.73 eV for Al(111),[10,22,23] while the experimental results are in the range 4.24–4.26 eV.[24–26] Similar discrepancies exist for the interlayer relaxations of the Al(111) and Al(100) surfaces.[23,27–32]

Nowadays, well-converged all-electron first-principles calculations for high- and low-Miller-index metal surfaces using a (1×1) surface unit cell can be performed in most personal computers. Therefore, the oscillatory behavior of the surface properties as function of the film thickness can be investigated in its full extension by taking into account a large number of layers in the slab, as well as a full relaxation of the interlayer spacings.

To obtain a further understanding of QSE in metal surfaces, as well as to investigate several discrepancies between first-principles calculations and experimental results for the low-Miller-index Al surfaces, in the present work we focused on the study of the dependence of the clean surface properties of the (111), (100), and (110) Al surfaces as a function of the film thickness. The following surface properties were studied: surface energy, work function, interlayer relaxations, total density of states at the Fermi level, and occupied bandwidth at the Γ point. The calculations are based on density-functional theory (DFT), employing the all-electron full-potential linearized augmented plane-wave (FLAPW) method. Due the high accuracy of the all-electron FLAPW method in solving the Khon-Sham equations, the results obtained in the present work can be used as a reference for further studies, e.g., semiempirical and pseudopotential calculations.

This paper is organized as follows: In Sec. II, the FLAPW method and computational details will be described. In Sec.

 ©2005 The American Physical Society

III, the surface properties of the Al surfaces will be presented and discussed. The QSE are discussed in Sec. IV, while in Sec. V we summarize the main conclusions obtained in the present work. Furthermore, test calculations are reported in the Appendix for the particular case of the Al(110) surface.

II. METHOD AND COMPUTATIONAL DETAILS

All calculations were performed using DFT[33,34] within the generalized gradient approximation (GGA) for the exchange-correlation (XC) energy functional.[35] The Kohn-Sham equations are solved using the all-electron FLAPW method,[36] as it is implemented in the FLEUR code.[37] The core states are treated fully relativistically, while the valence states are treated by the scalar relativistic approximation.

In the interstitial region the LAPW wave functions are represented using a plane-wave expansion truncated to include only plane-waves that have kinetic energies less than 9.00 Ry. The potential representation in the interstitial region in plane waves are truncated to include plane waves with kinetic energies less than 256 Ry. Inside the atomic spheres centered at the atom positions with radius $R_{mt}^{\mathrm{Al}}=1.22$ Å, the LAPW wave functions are expanded in radial functions times spherical harmonics up to $l_{max}=10$, while for the potential representation terms up to $\tilde{l}_{\max}=6$ are included in the expansion. For the evaluation of the nonspherical Hamiltonian matrix elements terms up to $l_{max}^{ns}=6$ were considered. The linearization energies were set to be in the center of gravity of the occupied part of the band with the respective character $(s,p,d,f,\ldots)$.

In the FLEUR code[37] solid surfaces are modeled using the film geometry suggested by Krakauer *et al.*,[38] i.e., a single slab is sandwiched between two semi-infinite vacua. The semi-infinite vacua are described by a product of two-dimensional (2D) plane waves and a z-dependent function. The 2D plane-wave functions are matched to the three-dimensional plane waves of the interstitial region at a distance of $\pm D/2$ from the center of the slab. In the present work, the parameter D was determined by the following relation: $D=(N_l-1)d_0+4R_{mt}^{\mathrm{Al}}$, where d_0 is the interlayer spacing of the unrelaxed Al surfaces and N_l is the number of layers in the slab.

The integrations over the surface Brillouin zone (BZ) of the (111), (100), and (110) Al surfaces were performed using a (30×30), (30×30), and (30×21) Monkhorst-Pack[39] meshes, respectively, which correspond to 450, 450, and 315 **k** points in the surface BZ, respectively. Only two symmetry operations (inversion and identity), were used in our calculations. The Fermi surface was broadening by the Fermi-Dirac distribution function with an artificial electronic temperature[36] of 54 meV (give as $k_{\mathrm{B}}T_{el}$). The total energy was corrected to $T_{el}=0$ K using the correction proposed by Gillan.[40]

The Al surfaces were simulated using a (1×1) surface unit cell and employing slabs with thicknesses of up to 32.50 Å, which correspond to 15, 17, and 23 layers for Al(111), Al(100), and Al(110), respectively. To take advantage of the inversion symmetry present in the Al surfaces, both sides of the slab were relaxed, which reduces the computational cost. All layers in the slab were relaxed, except the layer in the center of the slab. We assumed that the atoms are in the equilibrium positions when the force on each atom is smaller than 0.10 mRy/bohr. The dependence of the clean surface properties with respect to computational parameters are discussed in the Appendix.

III. RESULTS AND DISCUSSION

A. Bulk cohesive properties

The bulk Al was simulated using a tetragonal unit cell with two Al atoms. The equilibrium lattice constant, a_0, and the bulk modulus calculated at the equilibrium volume, B_0, were obtained by fitting the total energies of 17 regularly spaced volumes to Murnaghan's equation of state.[41] To determine the cohesive energy per atom, E_{coh}, a spin-polarized calculation for the free Al atom was performed using a cubic box with side length of 10.58 Å. We obtained $a_0=4.04$ Å (4.05 Å), $B_0=0.75$ Mbar (0.79 Mbar), $E_{coh}=-3.65$ eV (−3.39 eV). The numbers in parentheses are experimental results from Ref. 42, which are in excellent agreement with our results.

Furthermore, our results are in excellent agreement with other first-principles calculations.[43–46] For example, Khein *et al.*[43] employing the FLAPW method and a different approach for the GGA functional, obtained a lattice constant (bulk modulus) of 4.10 Å (0.73 Mbar), which are larger (smaller) than our results by 0.06 Å (0.02 Mbar). Fuchs *et al.*[46] employing also the FLAPW method and the same GGA used in the present work, obtained a lattice constant (bulk modulus) of 4.04 Å (0.78 Mbar). Pseudopotential plane-wave calculations performed by Favot and Dal Corso,[44] and Fuchs *et al.*[45] obtained a lattice constant (bulk modulus) of 4.06 Å (0.75 Mbar) and 4.05 Å (0.79 Mbar), respectively. The cohesive energy per atom reported in Refs. 44–46 are −3.52, −3.52, and −3.60 eV, respectively, while our cohesive energy is −3.65 eV.

B. Surface energy

The surface energy, σ_s, is defined as the energy (per surface atom or per unit area) needed to split an infinite crystal into two semi-infinite crystals along some chosen plane.[2] Thus, σ_s depends on the strength of the bonding and on the choice of the cleavage plane. The semi-infinite Al surfaces are modeled using a single slab with a finite number of layers, N_l. Using this approach, σ_s is given by

$$\sigma_s=\frac{1}{2}(E_{tot}^{slab}-N_lE_{tot}^{bulk}), \tag{1}$$

where E_{tot}^{slab} is the total energy of a slab with N_l layers (one atom per layer), while E_{tot}^{bulk} is the reference bulk total energy per atom. The factor $1/2$ takes into account that the top and bottom of the slab are equivalent. Thus, σ_s is a function of N_l, and, hence, surface energies calculated from Eq. (1) can be compared with experimental surface energies obtained from semi-infinite film only in the asymptotic regime (i.e., large values of N_l).

The central problem in calculating σ_s using first-principles calculations and employing Eq. (1) is in obtaining a reliable reference bulk total energy. In principle, the slab and bulk total energies can be calculated by two separated calculations using the same theoretical approach. However, using DFT within LDA and employing the full-potential linear muffin-tin orbital (FP-LMTO) method, Fiorentini and Methfessel[47] found that the surface energy of the Pt(100) surface calculated from two separated calculations decreases as a function of the number of layers in the slab (divergent behavior of σ_s), which is an unphysical and unexpected result.

This problem was recently discussed by Da Silva,[16] employing the FLAPW method as implemented in the WIEN code[48] and the repeated slab geometry. It was found that the surface energy of Cu(111) calculated from two separated self-consistent total energy calculations and using Eq. (1) converges as a function of the number of layers in the slab, which is expected. It was found that unconverged first-principles calculations with respect to the number of **k** points used to perform the integrations over the surface BZ determines the divergent behavior of σ_s as a function of N_l.

Da Silva[16] pointed out that similar quality integrations over the surface and bulk BZ are required to obtain converged surface energies, which is only obtained by using high dense **k**-point meshes in both calculations. Furthermore, the slab and bulk systems need to be treated using exactly the same basis function type and cutoff energies. In the present work, the Al surfaces are modeled using the single slab geometry.[38] Thus, the semi-infinite vacua on both sides of the single slab are described by plane-waves times exponential decay functions, which are not used in the description of the bulk system. Hence, the bulk and slab systems are not treated exactly with the same basis function type. Due to the different description of the bulk and slab systems, we found a small divergent behavior of the surface energy of Al(111) and Al(100) as a function of N_l, which was not found for Al(110). The surface energy of Al(111) and Al(100) are more sensitive to the numerical accuracies than of the Al(110) surface due to the smaller magnitude of the oscillations as function of the number of layers in the slab (see Table I).

Thus, to obtain consistent surface energies, the reference bulk total energy required in Eq. (1) need to be obtained using a different approach. In the limit of large values of N_l, the reference bulk total energy can be obtained by a linear fitting of the slab total energies, which was used in the present work to obtain E_{tot}^{bulk}. This approach was suggested in Ref. 47, which can be considered as an alternative approach to obtain E_{tot}^{bulk} for the cases in which the two separated total calculations approach cannot be applied. The reference bulk total energies obtained from the three set of data [i.e., (111), (100), and (110)] differ less than 0.50 meV between themselves. The average value was used in the present work, which differs by almost 7.50 meV from the reference bulk total energy obtained self-consistently, which explains the divergent behavior mentioned above. Furthermore, we found that the reference bulk total energy does not depend on the interlayer relaxations of the surface.

The surface energies for the unrelaxed and fully relaxed (111), (100), and (110) Al surfaces calculated as a function of the number of layers in the slab are summarized in Table I. The results are provided with three numbers to show the small differences between the surface energies. Furthermore, the surface energies are plotted in Fig. 1 as a function of the slab thickness, which helps to show that the oscillations (see below) have a similar period.

TABLE I. Surface energy given in electron-volts per surface atom of unrelaxed, σ_s^f, and fully relaxed, σ_s, Al surfaces as a function of the number of layers in the slab, N_l. $\sigma_s(\mathrm{J}/m^2)=F\times\sigma_s(\mathrm{eV/surface\ atom})$ where $F=2.266$, 1.963, and 1.388 for Al(111), Al(100), and Al(110), respectively.

N_l	$\sigma_s^f(111)$	$\sigma_s(111)$	$\sigma_s^f(100)$	$\sigma_s(100)$	$\sigma_s^f(110)$	$\sigma_s(110)$
2	0.360	0.356	0.540	0.508	0.776	0.714
3	0.348	0.348	0.489	0.486	0.699	0.699
4	0.376	0.375	0.487	0.482	0.674	0.662
5	0.370	0.368	0.484	0.480	0.704	0.689
6	0.364	0.363	0.475	0.475	0.764	0.745
7	0.367	0.366	0.479	0.478	0.747	0.733
8	0.363	0.362	0.483	0.481	0.718	0.706
9	0.359	0.358	0.485	0.483	0.707	0.698
10	0.363	0.362	0.494	0.492	0.729	0.718
11	0.366	0.365	0.483	0.481	0.743	0.730
12	0.363	0.361	0.488	0.485	0.732	0.719
13	0.362	0.361	0.483	0.480	0.723	0.712
14	0.366	0.365	0.482	0.480	0.727	0.716
15	0.365	0.364	0.485	0.483	0.740	0.728
16			0.482	0.480	0.740	0.728
17			0.486	0.484	0.729	0.718
18					0.726	0.714
19					0.730	0.719
20					0.739	0.728
21					0.737	0.729
22					0.732	0.721
23					0.728	0.717

The surface energy of Al(111) and Al(110) clearly oscillates periodically as a function of the slab thickness. There are cusps in the surface energy of Al(111) for slab thickness of 4.67, 11.66, 18.66, and 27.99 Å, i.e., almost every 7.00 Å. Similar behavior can be seen for Al(110), however, the cusps occur for slab thickness of 4.29, 11.43, 17.14, 24.29, and 31.43 Å. Thus, for Al(110), there are cusps almost every 7.15 Å. Thus, the period in the oscillations are almost the same for Al(111) and Al(110). Furthermore, the first cusp appears at almost the same slab thickness for both surfaces (see Fig. 1).

However, the same behavior is not clearly found for Al(100). For example, the first cusp in σ_s occurs for a slab thickness of almost 10.10 Å, while it is not clear the position of a second cusp due to the finite number of layers considered in our calculations. Furthermore, the amplitude of the oscillations are smaller compared to those found for Al(111) and Al(110), in particular by neglecting the result obtained with three layers slab. Thus, the present results indicate a

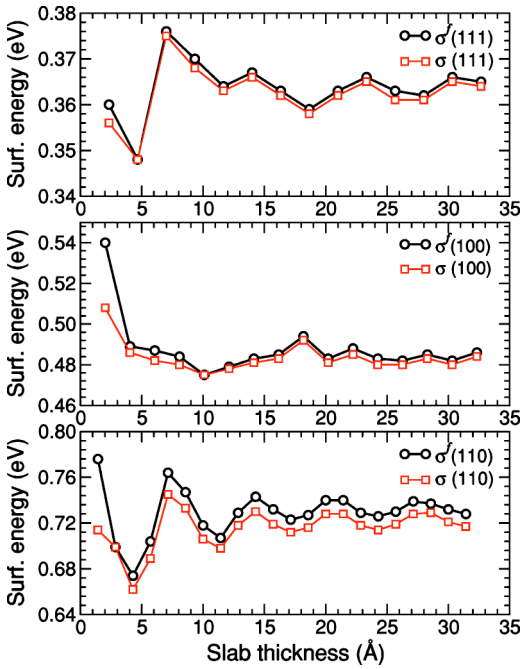

FIG. 1. (Color online) Surface energy per surface atom of the unrelaxed, σ_s^f, and fully relaxed, σ_s, (111), (100), and (110) Al surfaces as a function of the slab thickness.

different behavior for Al(100) compared with Al(111) and Al(110).

For both surfaces, the surface energy converges with respect to the number of layers in the slab, which is expected to be found but numerically difficult to be obtained using first-principles calculations. The surface energy decreases due to the energy gain in the interlayer relaxations, which is obtained in the calculations. For example, $\sigma_s^f - \sigma_s = 0.001$ eV (15 L), 0.002 eV (17 L), 0.011 eV (23 L) per surface atom for (111), (100), and (110), respectively. The large change in σ_s is obtained for Al(110), which is expected due to the larger magnitude of the relaxations compared to those found for Al(111) and Al(100). From now, the results obtained using the largest number of layers in the slab will be compared with published results, which are summarized in Table II.

Almost all surface energies summarized in Table II were calculated employing first-principles calculations within the local-density approximation (LDA). It has been known that the LDA functional overestimates cohesive energies and surface energies of metals in comparison with the GGA functional used in the present work.[46] Thus, it explains why our surface energies are smaller than those LDA results for all surfaces. For Al(111), our surface energy differs by 0.03 eV compared to the value reported by Da Silva[16] (0.33 eV), which was obtained using exactly the same GGA functional and method, however, a different implementation of the all-electron FLAPW method.[48] Surface energies calculated within the GGA functional, which are reported in Ref. 20, are larger than our results by 0.17, 0.21, and 0.20 eV for (111), (100), and (110) Al surfaces, respectively, i.e., a systematic overestimation compared to our results. These discrepancies might be due to the small number of **k** points and few layers used to model the surface, which was also discussed in Ref. 63.

TABLE II. A comparison of the calculated Al surface energies with published calculations and experimental results.

	Al(111)		Al(100)		Al(110)	
	(eV)	(J/m^2)	(eV)	(J/m^2)	(eV)	(J/m^2)
GGA	0.36[a]	0.82[a]	0.48[a]	0.94[a]	0.72[a]	1.00[a]
GGA	0.33[g]	0.75[g]				
GGA	0.53[h]	1.20[h]	0.69[h]	1.35[h]	0.92[h]	1.27[h]
LDA	0.39[g]	0.91[g]				
LDA	0.45[b]	1.27[i]			0.83[c]	
LDA	0.44[d]				0.77[f]	
LDA	0.48[e]		0.56[e]		0.89[e]	
Exp.		1.14[j]				

[a]Present work (fully relaxed slab).
[b]Reference 13.
[c]Reference 14.
[d]Reference 11.
[e]Reference 19.
[f]Reference 21.
[g]Reference 16.
[h]Reference 20.
[i]Reference 49.
[j]Reference 50.

The surface energy anisotropy ratios, which is given by $\sigma_s^*(hkl) = \sigma_s(hkl)/\sigma_s(111)$, can be better compared with the reported LDA results. We found $\sigma_s^* = 1.33$ and 1.97 for (100) and (110), respectively, while it is 1.17 (1.30) and 1.85 (1.74), respectively, using the results reported in Ref. 19 (Ref. 20). Thus, the agreement is not satisfactory, considering that we are comparing surface energy ratios calculated using first-principles calculations. Our anisotropy ratios are almost the same as those obtained from the number of broken bonds ratios, i.e., 1.33 and 2.00 for (100) and (110), respectively. Similar findings were recently reported in Ref. 63.

C. Work function

The work function, Φ, describes the ability of an electron to escape from a material, and it depends on the crystallographic orientation of the surface.[2] In periodic DFT calculations Φ is calculated as the difference between the total electrostatic potential at a point far from the surface and the Fermi energy, i.e., $\Phi = V_{es}(\infty) - E_F$. The work functions of the Al(111), Al(100), and Al(110) surfaces calculated as a function of the number of layers in the slab are summarized in Table III. Furthermore, the work functions are plotted in Fig. 2 as a function of the slab thickness to help in our discussion, as well as to stress the similar behavior of the oscillations. Φ^f and Φ indicate the work functions of frozen (unrelaxed) and relaxed slabs, respectively.

The multilayer relaxations change the work function of the low-Miller-index Al surfaces by a very *small* value, e.g., $\Phi^f - \Phi \approx 0.008$(15 L), 0.016 (17 L), and 0.003 eV (23) for

TABLE III. Work function given in elecron volt (eV) of unrelaxed, Φ^f, and fully relaxed, Φ, low-Miller-index Al surfaces as a function of the number of layers in the slab, N_l.

N_l	$\Phi^f(111)$	$\Phi(111)$	$\Phi^f(100)$	$\Phi(100)$	$\Phi^f(110)$	$\Phi(110)$
2	4.228	4.184	4.434	4.419	3.937	4.103
3	3.866	3.870	4.441	4.396	4.232	4.232
4	4.047	4.050	4.338	4.299	4.091	4.165
5	4.111	4.095	4.327	4.296	3.922	3.979
6	4.051	4.036	4.256	4.240	3.957	3.886
7	4.037	4.036	4.230	4.218	4.023	4.019
8	4.097	4.087	4.239	4.226	4.132	4.130
9	4.062	4.049	4.241	4.228	4.150	4.156
10	4.016	4.010	4.282	4.272	4.088	4.081
11	4.072	4.067	4.300	4.285	4.035	3.996
12	4.073	4.061	4.294	4.276	4.035	4.036
13	4.041	4.032	4.300	4.279	4.085	4.087
14	4.055	4.048	4.281	4.263	4.081	4.084
15	4.065	4.057	4.264	4.248	4.068	4.055
16			4.263	4.247	4.059	4.039
17			4.259	4.243	4.064	4.059
18					4.080	4.078
19					4.075	4.073
20					4.072	4.057
21					4.062	4.050
22					4.064	4.060
23					4.069	4.066

(111), (100), and (110), respectively. Thus, the largest change occurs for Al(100), which is an unexpected result due to the small magnitude of the relaxations of the topmost interlayer spacings of Al(100) compared with the larger relaxations of the Al(110) surface (see the next section). We found no clear trend in the changes of the work function due to the relaxations, i.e., an increase or decrease due to the relaxations. For example, for Al(111), $\Phi^f > \Phi$ for *all* studied slabs, except for $N_l = 3$ and 4, for which $\Phi^f < \Phi$. For Al(100), $\Phi^f > \Phi$ for *all* studied slabs. For Al(110), $\Phi^f > \Phi$ for most of the calculated slabs, however, $\Phi^f < \Phi$ for $N_l = 2$, 4, 5, 9, 12, 13, and 14. Thus, the relative changes depends strongly on the number of layers in the slab. Therefore, at least for the low-Miller-index Al surfaces, there is no clear relation between the magnitude of the topmost relaxations and the magnitude and sign of the work function changes.

Figure 2 shows a very similar periodic oscillatory behavior of the work functions of the Al(111) and Al(110) as a function of the slab thickness. For Al(110), there are minimums in the work function for a slab thickness of 1.43, 7.14, 14.28, 21.43, and 28.57 Å, i.e., one minimum for almost every 7.15 Å. A similar trend is also found for Al(111). However, these trends differ from those obtained for Al(100), in which the first minimum occurs for 12.12 Å. Furthermore, we found that the work function of the Al(111) and Al(110) for large slab thickness does not depend on the surface orientation, i.e., $\Phi(111) \approx \Phi(110)$, however, the same does not hold true for Al(100), e.g., $\Phi(100) - \Phi(111) \approx 0.20$ eV.

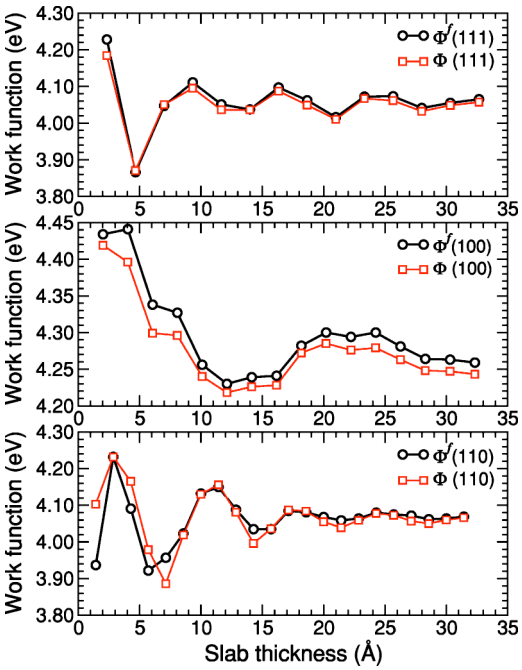

FIG. 2. (Color online) Work function of unrelaxed, Φ^f, and fully relaxed, Φ, (111), (100), and (110) Al surfaces as a function of the slab thickness.

From now, our well-converged work functions will be compared with experimental and first-principles results. There are only few theoretical work functions of the Al(100) and Al(110) surfaces available,[14,51] however, there are quite a large number of results for Al(111), in particular, employing the LDA functional[10,11,13,14,21–23,49,51] (see Table IV). The LDA work functions reported for Al(111) are in the range

TABLE IV. A comparison of FLAPW Al work functions (given in eV) with calculations and experimental results.

	Al(111)		Al(100)	Al(110)
GGA	4.06[a]		4.24[a]	4.07[a]
LDA	4.23[b]	4.73[c]	4.42[b]	4.12[d]
LDA	3.70[e]	4.59[f]		
LDA	4.09[g]	4.31[h]		
LDA	4.54[i]	4.32[j]		
Exp.	4.24±0.02[k]		4.41±0.03[k]	4.28±0.02[k]
Exp.	4.26±0.03[l]		4.20±0.03[l]	4.06±0.03[l]

[a]Present work (fully relaxed slab).
[b]Reference 51.
[c]Reference 22.
[d]Reference 14.
[e]Reference 11.
[f]Reference 13.
[g]Reference 23.
[h]Reference 10.
[i]Reference 49.
[j]Reference 21.
[k]Reference 24.
[l]Reference 25.

from 3.70–4.73 eV, which indicates a large discrepancy between the first-principles calculations. It has been know that in general LDA work functions are larger than those calculated using GGA functionals,[16] hence, it explains the fact that the work functions calculated in the present work are smaller than most of the LDA results. Hence, our GGA results cannot be compared directly with the LDA results, however, the relative differences can be compared. For example, we found that $\Phi(100)-\Phi(111)=0.18$ eV, which is good agreement with the LDA value of 0.19 eV reported in Ref. 51.

Our converged work functions differ by 0.18, 0.17, and 0.21 eV compared with experimental photoelectric measurements carried out in ultrahigh vacuum conditions[24] for Al(111), Al(100), and Al(110), respectively (see Table IV). Furthermore, $\Phi(100)-\Phi(111)=0.17$ eV and $\Phi(111)\approx\Phi(110)$, which are in excellent agreement with our results. Photoelectric experiments reported in Ref. 25 obtained $\Phi(111)\approx\Phi(100)$ and $\Phi(111)-\Phi(110)=0.20$ eV, which are in clear disagreement with our results, as well as with the experimental results reported in Ref. 24. Grepstad *et al.*[24] suggested that impurities, in particular oxygen, might be the reason for those discrepancies.[26] As reported in Ref. 24, special care was taken with the cleanliness of the Al surfaces, hence, these results are considered as a reference for our theoretical calculations.

D. Multilayer relaxations

The interlayer relaxations, $\Delta d_{i,i+1}$, are given in percent with respect to the unrelaxed interlayer spacings, d_0, i.e., $\Delta d_{i,i+1}=100(d_{i,i+1}-d_0)/d_0$. $d_{i,i+1}$ is the interlayer distance between two adjacent layers parallel to the surface calculated by total energy minimization. $d_0=a_0\sqrt{3}/3, a_0/2$, and $a_0\sqrt{2}/4$ for (111), (100), and (110), respectively. Hence, the signs + and − signs indicate expansion and contraction of the interlayer spacings, respectively. All layers in the slab were allowed to relax, except the layer in the center of the slab, however, only the relaxations of the topmost six interlayer spacings $(d_{12},\ldots,d_{67})$ will be discussed due to the small magnitude of the relaxations of the inner interlayer spacings. It does not change the conclusions obtained in the present work. The relaxations of the (111), (100), and (110) Al surfaces as a function of the number of layers in the slab, N_l, are summarized in Tables V–VII, respectively. Furthermore, the relaxations are also plotted in Fig. 3 to help in our discussion.

For Al(111) and Al(100), in which there are three and four broken bonds in the surface, respectively, the topmost interlayer spacing, d_{12}, expands by few percent for all calculated slabs, except for Al(111) using $N_l=3$. For Al(110), in which there are six broken bonds in the surface, d_{12} contracts for all calculated slabs. For both surfaces, the magnitude of the relaxations show a periodic oscillatory behavior as a function of N_l. For Al(111), the expansion of the topmost interlayer spacing as a function of the number of layers in the slab shows a minimum for $N_l=3$, 7, 10, and 13, i.e., a minimum for almost every three interlayer spacings (7.00 Å). Furthermore, it can be seen in Fig. 3 that the topmost six interlayer relaxations show similar behavior. For Al(110), the contraction of the topmost interlayer spacing has a maximum for $N_l=6$, 11, 16, and 21, i.e., a maximum for almost every five interlayer spacings (7.14 Å). Further interlayer relaxations show a similar trend.

TABLE V. Relaxations given in percent, $\Delta d_{i,i+1}$, of Al(111) as a function of the number of layers in the slab, N_l.

N_l	Δd_{12}	Δd_{23}	Δd_{34}	Δd_{45}	Δd_{56}	Δd_{67}
2	+3.679					
3	−0.182					
4	+1.246	−0.482				
5	+1.796	+0.677				
6	+1.084	−0.017	+0.780			
7	+0.901	−0.472	+0.463			
8	+1.411	+0.106	+0.608	+0.600		
9	+1.180	−0.041	+0.476	+0.161		
10	+0.854	−0.420	+0.260	−0.059	−0.413	
11	+1.278	−0.001	+0.582	+0.347	−0.006	
12	+1.235	−0.003	+0.574	+0.295	+0.047	+0.027
13	+1.001	−0.246	+0.354	+0.038	−0.265	−0.120
14	+1.100	−0.168	+0.395	+0.148	−0.214	−0.181
15	+1.151	−0.053	+0.456	+0.215	−0.049	−0.057

The oscillatory behavior found for Al(111) and Al(110) are very similar, however, different from those obtained for Al(100). For Al(100), the expansion of the topmost interlayer spacing has the first minimum for $N_l=6$, however, a second minimum is not clearly obtained considering N_l up to 17. These results show that the period of the oscillations are different by a large value between the Al(100) surface and the (111) and (110) Al surfaces. A similar trend was also found for the surface energy and work function. From now,

TABLE VI. Relaxations given in percent, $\Delta d_{i,i+1}$, of Al(100) as a function of the number of layers in the slab, N_l.

N_l	Δd_{12}	Δd_{23}	Δd_{34}	Δd_{45}	Δd_{56}	Δd_{67}
2	+4.344					
3	+2.558					
4	+2.481	+2.136				
5	+2.394	+1.899				
6	+1.122	+0.153	+0.255			
7	+1.477	−0.057	−0.571			
8	+1.421	+0.420	−0.450	−1.169		
9	+1.535	+0.432	−0.019	−0.894		
10	+1.900	+0.838	+0.373	−0.160	−0.326	
11	+1.685	+0.849	+0.436	−0.106	−0.018	
12	+1.961	+0.866	+0.526	−0.058	+0.144	+0.424
13	+1.853	+0.996	+0.359	−0.085	+0.070	+0.356
14	+1.649	+0.557	+0.255	−0.492	−0.299	+0.030
15	+1.600	+0.549	+0.016	−0.429	−0.398	+0.014
16	+1.596	+0.592	+0.071	−0.656	−0.373	−0.150
17	+1.598	+0.436	−0.020	−0.682	−0.564	−0.085

TABLE VII. Relaxations given in percent, $\Delta d_{i,i+1}$, of Al(110) as a function of the number of layers in the slab, N_l.

N_l	Δd_{12}	Δd_{23}	Δd_{34}	Δd_{45}	Δd_{56}	Δd_{67}
2	−28.312					
3	−0.048					
4	−7.777	+7.656				
5	−6.222	−0.138				
6	−10.360	+5.853	−6.308			
7	−8.332	+5.057	−0.243			
8	−6.542	+4.329	−0.603	+4.319		
9	−5.661	+2.927	−1.297	+2.825		
10	−6.922	+3.278	−2.978	+1.743	+0.940	
11	−8.179	+3.929	−2.874	+0.903	−0.069	
12	−7.986	+4.439	−2.035	+1.980	+0.077	+0.212
13	−6.822	+3.915	−1.570	+2.322	+1.000	+0.003
14	−6.751	+3.615	−2.263	+2.244	+1.047	+0.227
15	−7.303	+3.637	−2.422	+1.506	+0.734	+0.148
16	−7.816	+4.164	−2.297	+1.840	+0.169	+0.334
17	−7.345	+4.087	−1.868	+2.009	+0.640	+0.109
18	−7.127	+3.933	−2.047	+2.068	+0.680	+0.346
19	−6.971	+3.705	−2.260	+1.819	+0.692	+0.139
20	−7.472	+4.023	−2.432	+1.733	+0.499	+0.151
21	−7.583	+4.071	−2.140	+1.804	+0.393	+0.047
22	−7.410	+3.937	−2.151	+1.939	+0.337	+0.027
23	−7.180	+3.873	−2.123	+2.044	+0.816	+0.222

the results obtained using the largest number of layers in the slab will be compared with experimental results, as well as with published calculations.

1. Al(111)

The topmost interlayer spacing expands by +1.15% (≈0.03 Å). This result is in good agreement with two quantitative low-energy electron diffraction (LEED) studies, which obtained expansions of +0.9±0.5%,[28] and +1.4±0.5%.[30] However, our results differs significantly from other two LEED studies, which reported expansions of $\Delta d_{12}=+2.2\%$,[27] and +1.7±0.3%.[29] The LEED intensities reported in Refs. 28 and 29 were obtained at a temperature of 90 K and 160 K, respectively, which migh explains the difference in the magnitude of the relaxations. We found a contraction of only −0.05% for the second interlayer spacing, i.e., $d_{12}\approx d_0$, however, LEED studies[29] obtained an expansion of +0.5±0.7%. Indeed, such an expansion is obtained in our calculations using a slab with five layers, but this results is not converged with respect to the number of layers in the slab. The error in the LEED result for d_{23} reported in Ref. 29 is larger than the value itself. The third interlayer spacing expands by +0.46%(≈0.01 Å). There are no LEED results for d_{34}.

Our result for the topmost interlayer spacing is in good agreement with some first-principles calculations, e.g., +1.06%,[23] +1.38%,[52] +1.18%,[53] however, is in disagreement with the large expansion, e.g., +2.0%, reported in Ref. 32.

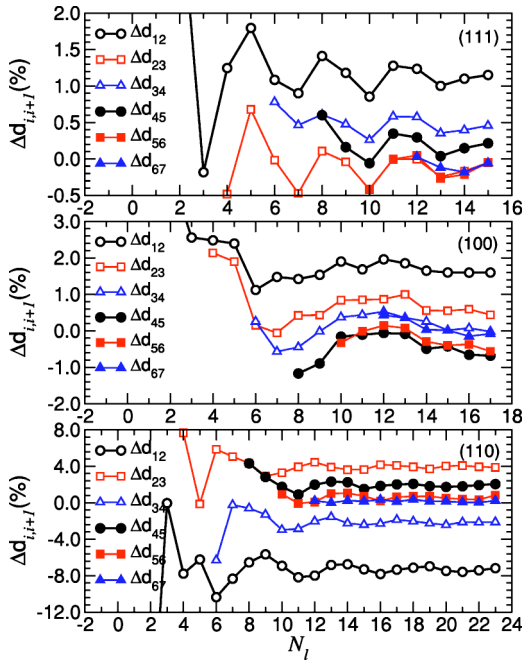

FIG. 3. (Color online) Relaxations, $\Delta d_{i,i+1}$, of the (111), (100), and (110) Al surfaces as a function of the number of layers in the slab, N_l.

Furthermore, there are large discrepancies in the magnitude of the relaxations for the second and third interlayer spacings compared with our results. For example, $\Delta d_{23}=-1.53\%$,[23] −2.14%,[52] −0.40%,[53] while $\Delta d_{34}=-0.54\%$,[23] +1.08%,[52] +0.20%.[53] The number of layers in the slab plays a role in the magnitude of the relaxation of the second and third interlayer spacings, however, it is not enough to explains the discrepancies discussed above.

2. Al(100)

For Al(100), the topmost two interlayer spacing expands by few percent, e.g., $\Delta d_{12}=+1.60\%$ and $\Delta d_{23}=+0.44\%$. Almost three decades ago,[54,27] a quantitative analysis of LEED intensities measured at 300 K found $\Delta d_{12}\approx 0$ (no relaxation), which is in clear disagreement with our results. However, recent LEED studies[31] performed at a temperature of 100 K obtained $\Delta d_{12}=+2.0\pm0.8\%$ and $\Delta d_{23}=+1.2\pm0.7\%$, which are in better agreement with our results considering the large errors in the LEED results.

First-principles calculations reported in Ref. 55 obtained an expansion of +1.2±0.4% for d_{12}, which is close to our result, however, recent first-principles calculations[32] found an expansion of +0.5% for d_{12}, which is smaller than our result. Furthermore, a contraction of −0.3% was found for d_{23} (Ref. 32), which is in clear disagreement with our results reported in Table VI, as well as with LEED results.[31]

3. Al(110)

The first and third interlayer spacings contract by −7.18% and −2.12%, respectively, while the second interlayer spacing expands by +3.87%. We found an interlayer relaxation-sequence like $-+-+++\cdots$. There is a clear alternate sign in

TABLE VIII. A comparison of the relaxations of the Al(110) surface with LEED and theoretical results.

Method Reference	Temp. (K)	Δd_{12} (%)	Δd_{23} (%)	Δd_{34} (%)	Δd_{45} (%)	Δd_{56} (%)
FLAPW[a]	0	−7.18	+3.87	−2.12	+2.04	+0.82
PPPW[21]	0	−7.0	+3.4	−2.4	+1.6	
PPPW[57]	0	−7.4	+3.8	−2.5	+2.0	
PPPW[14]	0	−6.9				
LEED[54]	100	−8.6	+5.0	−1.6		
LEED[53]	100	−8.4	+4.9	−1.6	+0.2	
LEED[55]	100	−8.1	+5.5	−3.8	+1.1	
LEED[55]	300	−11.2	+6.7	−4.0	0.0	
LEED[61]	297	−8.5	+5.5	+2.2	+1.6	
LEED[58]	70	−6.9	+4.1	−3.7		
LEED[58]	316	−7.6	+5.0	−3.2		

[a]Present work.

the relaxations for the topmost four interlayer spacings, however, it does not hold true for inner interlayer spacings due to the expansion of the fifth interlayer spacing. The magnitude of the relaxations decrease for inner interlayer spacings, i.e., $|\Delta d_{i,i+1}| > |\Delta d_{i+1,i+2}|$.

The magnitude and sign of the relaxations are in good agreement with available LEED studies[56–60] (see Table VIII). However, there are discrepancies for particular cases. For example, LEED results reported in Ref. 60 found an expansion of +2.2% for d_{34}, while we found that d_{34} contracts by −2.12%. It can be noted in Table VIII that several LEED studies[56–59] obtained a contraction for d_{34}, which is in agreement with our result. Furthermore, our results are in excellent agreement with published first-principles calculations,[21,14,61] as can be seen in Table VIII. It is important to note that temperature effects increase the contraction of the topmost interlayer spacing, which was recently discussed in Ref. 58. In fact the LEED results obtained at a temperature of 70 K are in better agreement with our results than those obtained at 316 K.

E. Total density of states

Our results for the total density of states (DOS) are summarized in Fig. 4. For a system with two-dimensional periodicity, it can be shown that a single parabolic band, i.e., a slab with a single atomic layer, produces a step-like function DOS.[18] If an extra layer is added in the slab, then it generates an additional step in the DOS. This behavior is precisely shown in Fig. 4 for a slab with two layers for the (111), (100), and (110) Al surfaces. The number of steps increases with increasing the number of layers in the slab, which is difficult to be seen using slabs with a larger number of layers, e.g., $N_l > 8$ (see Fig. 4).

The total DOS calculated using slabs with 8 and 15 layers for Al(111) are almost identical, except in the region close to the Fermi energy (see Fig. 4). Motivated by this observation, the total DOS calculated at the Fermi energy, DOS(E_F), was calculated as a function of the slab thickness. DOS(E_F) for

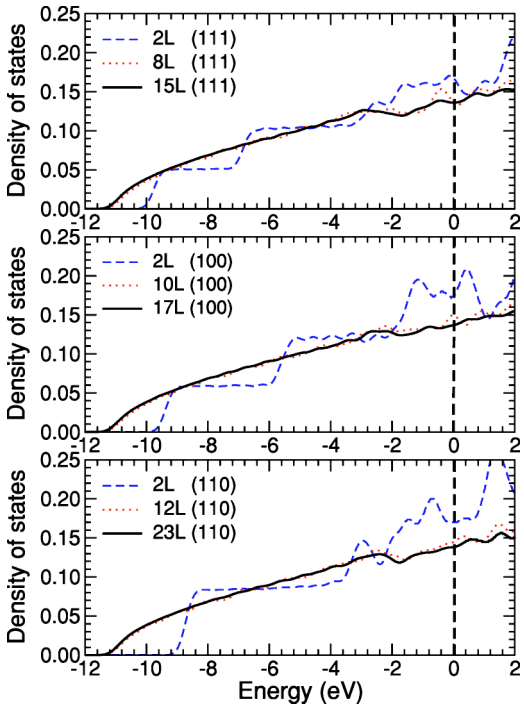

FIG. 4. (Color online) Total density of states (DOS) of the fully relaxed (111), (100), and (110) Al surfaces for a different number of layers in the slab. The vertical dashed lines indicate the Fermi energy. The total DOS are normalized to unity, i.e., the integral of the DOS up to the Fermi energy is set to unity.

(111), (100), and (110) Al surfaces are plotted in Fig. 5. The changes in the total DOS at the Fermi energy due to the relaxation of the layers are almost negligible for slabs with a larger number of layers, however, small differences can be noted for slabs with few atomic layers.

For Al(110), it can be seen in Fig. 5 that DOS(E_F) calculated as a function of the slab thickness shows a periodic oscillatory behavior as function of the slab thickness. For example, there are minimums in the DOS calculated at the Fermi energy for slabs with 5, 9, 13, and 18 layers. Similar behavior was found for the surface energy, work function, and multilayer relaxations. A similar trend is found for the surface properties of the Al(111) and Al(100) surfaces. Therefore, our results indicate that the changes in the density of states at the Fermi energy as a function of the slab thickness might originate changes in the surface energy, work function, and multilayer relaxations.

F. Occupied bandwidth at Γ point

The occupied bandwidth at the Γ point, W_Γ, of the (111), (100), and (110) slabs was calculated as the difference between the Fermi energy and the lowest occupied eigenvalue at the Γ point. The results are summarized in Fig. 6. There are no oscillations in the magnitude of W_Γ as a function of the number of layers in the slab, as those found for the surface energy, work function, multilayer relaxations. We found that 8, 8, and 11 layers in the slab are enough to obtain W_Γ that differ by less than 1.00% compared with results calcu-

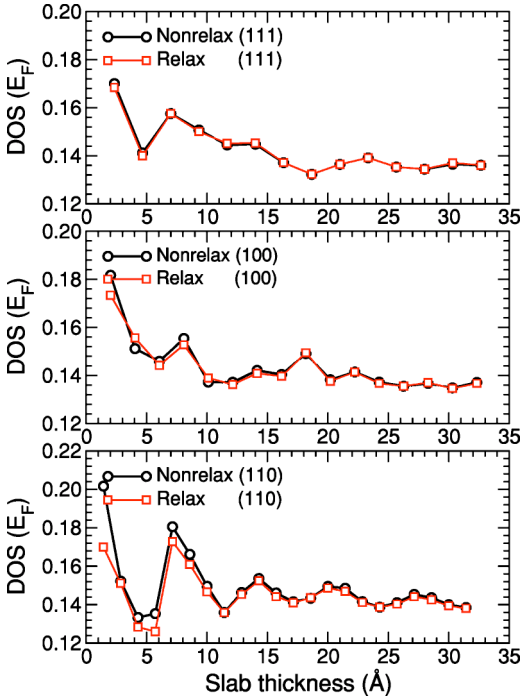

FIG. 5. (Color online) Total density of states (DOS) calculated at the Fermi energy, DOS(E_F), of the unrelaxed and fully relaxed (111), (100), and (110) Al surfaces as a function of the number of layers in the slab. The total DOS are normalized to unity, i.e., the integral of the DOS up to the Fermi energy is set to unity.

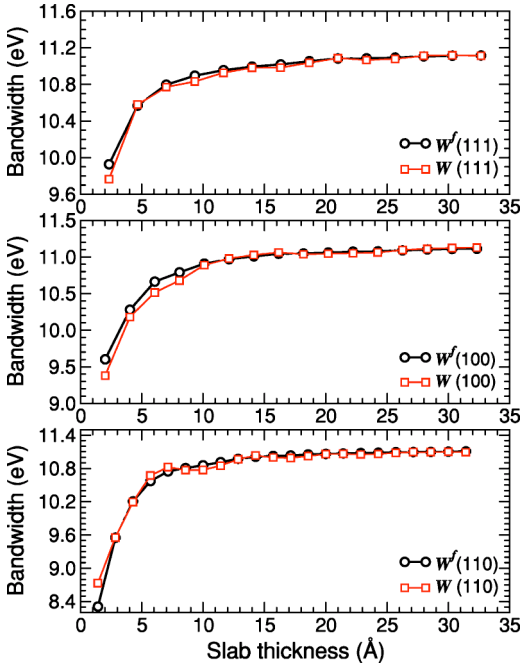

FIG. 6. (Color online) Occupied bandwidth at the Γ point of unrelaxed, W_Γ^f, and fully relaxed, W_Γ, (111), (100), and (110) Al surfaces as a function of the slab thickness.

lated with 15, 17, and 23 layers in the slab for (111), (100), and (110), respectively.

IV. QUANTUM-SIZE EFFECTS

Our results show a periodic oscillatory behavior of the surface energies, work functions, multilayer relaxations, and density of states as a function of the slab thickness for the (111), (100), and (110) Al surfaces. These oscillations have been discussed and attributed to QSE in several studies.[1,10–18] However, the results obtained in the present work cannot be fully explained based only on the old picture suggested in Ref. 1. For example, based on jellium film calculations,[1] Schulte found that the work function show oscillations with a period of roughly one-half of the Fermi wavelength, λ_F (λ_F = 3.58 Å for Al).

We found that the surface energies, work functions, multilayer relaxations, and total DOS calculated at the Fermi level have similar oscillatory behavior as a function of the slab thickness for Al(111) and Al(110), e.g., for Al(111), there is a cusp in the plots at almost every 7.00 Å, while it is 7.15 Å for Al(110). Hence, the period of the oscillations are almost the same for Al(111) and Al(110), which is almost two times larger than those suggested by Schulte. However, a different physical behavior was found for Al(100). The work functions and multilayer relaxations results indicate a larger distance between two consecutive cusps compared to those found for Al(111) and Al(110). It can be seen in Fig. 2 that two consecutive cusps are separated by almost 12.12 Å, i.e., almost 3.38 times the Fermi wavelength of the bulk aluminum.

Therefore, we found that the same value of the Fermi wavelength cannot be correlated with the distance between two cusps in the clean surface properties for the low-Miller-index Al surfaces. This result was not identified in the Schulte's jellium calculations, since it did not take into account the atomic structure of the surfaces, as well as was not identified in recent first-principles calculations. As a consequence of the larger oscillatory period found for Al(100), a larger number of layers would be required to obtain well-converged results for Al(100). However, this is not the case for most of the studied properties due to the small magnitude of the oscillations as a function of the number of layers compared to the oscillations found for Al(110).

The different behavior of the surface properties of Al(100) compared to the Al(111) and Al(110) surfaces can be explained by the findings reported in Ref. 62 for Al(100). For example, the occupied surface states of the Al(100) surface has a deep penetration into the bulk region according to Ref. 62, which might originate oscillations with a larger period due to the increase in the occupation of the surface states.

V. SUMMARY

Systematic DFT calculations, employing the FLAPW method, were performed for the clean Al(111), Al(100), and Al(110) surfaces. The surface energies, work functions, interlayer relaxations, density of states, and occupied bandwidth at the Γ point were calculated as a function of the slab thickness up to 32 Å. Due to the high accuracy of the all-electron FLAPW method in solving the Kohn-Sham equa-

TABLE IX. Surface energy, σ_s, work function, Φ, and interlayer relaxations, $\Delta d_{i,i+1}$, of the Al(110) surface calculated as a function of the cutoff energy, K^{wf}, and the number of **k** points in the surface BZ, $N_{\mathrm{BZ}}^{\mathbf{k}}$. σ_s^f and Φ^f indicate the surface energy and work function calculated for unrelaxed slabs, respectively.

K^{wf} (Ry)	$N_{\mathrm{BZ}}^{\mathbf{k}}$	**k** points mesh	σ_s^f (eV)	σ_s (eV)	Φ^f (eV)	Φ (eV)	Δd_{12} (%)	Δd_{23} (%)	Δd_{34} (%)	Δd_{45} (%)	Δd_{56} (%)	Δd_{67} (%)
5.06	70	(14×10)	0.714	0.697	4.071	4.063	−6.366	+4.552	−1.058	+3.517	+2.605	+0.796
6.25	70	(14×10)	0.752	0.741	4.069	4.077	−6.927	+3.676	−1.982	+2.133	+1.301	−0.136
7.56	70	(14×10)	0.755	0.743	4.069	4.080	−7.024	+3.527	−2.142	+1.981	+1.196	−0.299
9.00	70	(14×10)	0.756	0.744	4.069	4.080	−7.054	+3.499	−2.146	+1.981	+1.141	−0.305
10.56	70	(14×10)	0.757	0.745	4.069	4.081	−7.066	+3.512	−2.172	+1.949	+1.154	−0.330
12.25	70	(14×10)	0.757	0.745	4.069	4.080	−7.056	+3.434	−2.171	+1.986	+1.071	−0.300
14.06	70	(14×10)	0.757	0.745	4.069	4.080	−7.078	+3.487	−2.160	+1.986	+1.098	−0.305
16.00	70	(14×10)	0.757	0.745	4.069	4.080	−7.083	+3.487	−2.154	+1.988	+1.096	−0.304
10.56	6	(4×3)	1.488	1.440	4.081	3.961	−6.851	+0.734	−4.341	−5.067	−1.503	−3.422
10.56	12	(6×4)	0.707	0.685	3.991	3.981	−7.270	+6.256	−3.488	+6.375	+0.057	+1.505
10.56	24	(8×6)	0.682	0.672	4.106	4.092	−6.218	+4.135	+0.112	+0.659	+1.528	+1.115
10.56	35	(10×7)	0.674	0.658	4.074	4.068	−7.559	+3.134	−2.882	+1.172	+1.800	−1.238
10.56	48	(12×8)	0.691	0.680	4.066	4.066	−6.996	+4.045	−1.527	+2.969	+0.615	+0.168
10.56	70	(14×10)	0.757	0.745	4.069	4.081	−7.066	+3.512	−2.172	+1.949	+1.154	−0.330
10.56	88	(16×11)	0.738	0.727	4.108	4.105	−6.862	+4.388	−1.327	+2.528	+0.770	−0.656
10.56	117	(18×13)	0.723	0.710	4.082	4.080	−7.126	+4.140	−1.892	+2.481	+1.207	+0.147
10.56	140	(20×14)	0.710	0.701	4.075	4.075	−6.291	+3.619	−1.380	+2.359	+1.307	−0.332
10.56	176	(22×16)	0.711	0.701	4.079	4.081	−6.791	+3.812	−1.293	+2.435	+1.083	−0.073
10.56	204	(24×17)	0.719	0.708	4.084	4.087	−7.025	+3.990	−1.960	+2.322	+0.809	−0.108
10.56	234	(26×18)	0.714	0.704	4.081	4.081	−6.520	+3.811	−1.560	+2.148	+1.093	−0.075
10.56	280	(28×20)	0.720	0.710	4.081	4.085	−6.718	+3.830	−1.621	+1.946	+1.076	−0.197
10.56	315	(30×21)	0.718	0.708	4.085	4.087	−6.821	+3.926	−1.584	+2.300	+0.963	−0.062
10.56	368	(32×23)	0.716	0.706	4.077	4.079	−6.735	+3.778	−1.649	+2.316	+1.048	−0.045
10.56	408	(34×24)	0.719	0.709	4.081	4.083	−6.765	+3.910	−1.578	+2.274	+1.006	−0.099
10.56	450	(36×25)	0.718	0.708	4.082	4.084	−6.764	+3.910	−1.634	+2.312	+1.035	−0.115

tions, our well-converged results can be considered as a database for the parametrization of empirical potentials, as well as a reference for the construction of pseudopotentials.

The mentioned surface properties, except the occupied bandwidth, oscillates as a function of the slab thickness, which is not a new result. However, we found that the period of those oscillations are not the same for all studied Al surfaces, which has not been reported before. In particular, the period of the oscillations are almost the same for Al(111) and Al(110), however, it differs significantly for Al(100), in which the oscillations have a larger period. These results are explained by the findings reported in Ref. 62. For example, the occupied surface states of the Al(100) surface has a deep penetration into the bulk region, which might originate oscillations with a larger period. These trends were found for unrelaxed and fully relaxed slabs.

Furthermore, our results indicate that the surface energy anisotropy ratios are closer to the ideal anisotropy ratios calculated from the number of broken bond ratios. Hence, the surface energy of other Al surfaces can be calculated as a first approximation from the number of broken bonds in the surface. We found that the work function of the Al(111) and Al(110) surfaces are almost exactly the same for slabs with a large number of layers, while the work function of Al(100) is larger by $\approx$0.20 eV, which is in good agreement with experimental results.

The magnitude of the interlayer relaxations obtained for Al(111) and Al(100) are not in good agreement with published theoretical calculations, in particular, for the inner interlayer spacings. The differences cannot be explained in terms of the number of layers in the slab. However, the relaxations obtained for Al(110) are in good agreement with first-principles calculations. In general, our multilayer relaxations are in good agreement with quantitative LEED intensity analysis.

ACKNOWLEDGMENTS

We thank the Institute of Solid State Physics of the Research Center Jülich for the computer time (DEC-Cluster) to perform the present work. We are also thankful for the comments from the referees on the present paper.

APPENDIX:

Here, we will discuss the dependence of σ_s, Φ, and $\Delta d_{i,i+1}$ of Al(110) as a function of computational parameters. The

calculations were performed for eight cutoff energies (K^{wf} = 5.06, …, 16.00 Ry), and for 17 set of **k** points ($N^{\mathbf{k}}_{\mathrm{BZ}}$ = 6, …, 450) using a slab with 13 layers. All results are summarized in Table IX. The results obtained with the largest computational parameters will be used as a reference in the discussion below.

A cutoff energy of 6.25 Ry (5.06 Ry) is enough to obtain surface energies (work functions) that differ less than 0.65% (0.50%) compared with the converged results. To obtain a similar level of convergence for $\Delta d_{i,i+1}$, i.e., error smaller than 1.00%, a cutoff energy of 9.00 Ry is required. We found that the values of σ_s, Φ, and $\Delta d_{i,i+1}$ oscillates as a function of the number of **k** points. These oscillations decrease with an increase in the number of **k** points. We found that at least 176 (24) **k** points in the surface BZ are required to obtain surface energies (work functions) that differ less than 1.00% compared with the converged results. However, to obtain absolute values for Δd_{12} and Δd_{23} that differ less than 1.00% compared to the converged results, 315 **k** points are required, while a larger number of **k** points, e.g., 368, are required to obtain similar accuracy for the relaxations of the inner interlayer spacings. Hence, the multilayer relaxations of Al(110) are very sensitive to the number of **k** points, while converged work functions can be calculated using few **k** points.

Therefore, we concluded that a cutoff energy of 9.00 Ry and 315 **k** points in the surface BZ, i.e., a (30×22) two-dimensional **k** point mesh, are enough to obtain well-converged σ_s, Φ, and $\Delta d_{i,i+1}$ for Al(110). The same cutoff energy and similar high quality two-dimensional **k** point meshes were used for the calculations of the (111) and (100) Al surfaces.

*Present address: Humboldt-Universitaet zu Berlin, Institut fuer Chemie Arbeitsgruppe Quantenchemie, Unter den Linden 6 D-10099 Berlin, Germany. Electronic address: dasilvaj@chemie.hu-berlin.de

[1] F. K. Schulte, Surf. Sci. **55** 427 (1976).
[2] M.-C. Desjonquères and D. Spanjaard, *Concepts in Surface Science* (Springer-Verlag, Berlin, 1995).
[3] T. Miller, S. Samsavar, G. E. Franklin, and T. C. Chiang, Phys. Rev. Lett. **61**, 1404 (1988).
[4] J. E. Ortega, F. J. Himpsel, G. J. Mankey, and R. F. Willis, Phys. Rev. B **47**, 1540 (1993).
[5] M. Jalochowski, E. Bauer, H. Knoppe, and G. Lilienkamp, Phys. Rev. B **45**, 13 607 (1992).
[6] M. Jalochowski, Prog. Surf. Sci. **48**, 287 (1995).
[7] M. Jalochowski, M. Hoffman, and E. Bauer, Phys. Rev. Lett. **76**, 4227 (1996).
[8] J. A. Kubby, Y. R. Wang, and W. J. Greene, Phys. Rev. Lett. **65**, 2165 (1990).
[9] M. S. Altman, W. F. Chung, Z. Q. He, H. C. Poon, and S. Y. Tong, Appl. Surf. Sci. **169**, 82 (2001).
[10] P. J. Feibelman and D. R. Hamann, Phys. Rev. B **29**, 6463 (1984).
[11] I. P. Batra, S. Ciraci, G. P. Srivastava, J. S. Nelson, and C. Y. Fong, Phys. Rev. B **34** 8246 (1986).
[12] S. Ciraci and I. P. Batra, Phys. Rev. B **33**, 4294 (1986).
[13] J. C. Boettger, Phys. Rev. B **53** 13 133 (1996).
[14] A. Kiejna, J. Peisert, and P. Scharoch, Surf. Sci. **432**, 54 (1999).
[15] G. Materzanini, P. Saalfrank, and P. J. D. Lindan, Phys. Rev. B **63**, 235405 (2001).
[16] J. L. F. Da Silva, *The Nature and Behavior of Rare-Gas Atoms on Metal Surfaces*, Ph.D. thesis, http://edocs.tu-berlin.de/diss/2002/dasilva_juarez.htm or http://www.fhi-berlin.mpg.de/th/pub02.html, Technical University Berlin, Berlin, Germany, 2002.
[17] C. M. Wei and M. Y. Chou, Phys. Rev. B **66**, 233408 (2002).
[18] J. C. Boettger and S. B. Trickey, Phys. Rev. B **45**, 1363 (1992).
[19] R. Stumpf and M. Scheffler, Phys. Rev. Lett. **72**, 254 (1994).
[20] L. Vitos, A. V. Ruban, H. L. Skriver, and J. Kollár, Surf. Sci. **411**, 186 (1998).
[21] K. M. Ho and K. P. Bohnen, Phys. Rev. B **32**, 3446 (1985).
[22] D.-S. Wang, A. J. Freeman, H. Krakauer, and M. Posternak, Phys. Rev. B **23**, 1685 (1981).
[23] A. Kiejna and B. I. Lundqvist, Phys. Rev. B **63**, 085405 (2001).
[24] J. K. Grepstad, P. O. Gartland, and B. J. Slagsvold, Surf. Sci. **57**, 348 (1976).
[25] R. M. Eastment and C. H. B. Mee, J. Phys. F: Met. Phys. **3**, 1738 (1973).
[26] P. O. Gartland, Surf. Sci. **62**, 183 (1977).
[27] F. Jona, D. Sondericker, and P. M. Marcus, J. Phys. C **13**, L155 (1980).
[28] H. B. Nielsen and D. L. Adams, J. Phys. C **15**, 615 (1982).
[29] J. R. Noonan and H. L. Davis, J. Vac. Sci. Technol. A **8**, 2671 (1990).
[30] J. Burchhardt, M. M. Nielsen, D. L. Adams, E. Lundgren, and J. N. Andersen, Phys. Rev. B **50**, 4718 (1994).
[31] J. H. Petersen, A. Mikkelsen, M. M. Nielsen, and D. L. Adams, Phys. Rev. B **60**, 5963 (1999).
[32] M. Borg, M, Birgersson, M. Smedh, A. Mikkelsen, D. L. Adams, R. Nyholm, C.-O. Almbladh, and J. N. Andersen, Phys. Rev. B **69**, 235418 (2004).
[33] P. Hohenberg and W. Kohn, Phys. Rev. **136**, B864 (1964).
[34] W. Kohn and L. J. Sham, Phys. Rev. **140**, A1133 (1965).
[35] J. P. Perdew, S. Burke, and M. Ernzerhof, Phys. Rev. Lett. **77**, 3865 (1996).
[36] D. J. Singh, *Plane Waves, Pseudopotentials and LAPW Method* (Kluwer Academic Publishers, Boston, 1994).
[37] http://www.flapw.de
[38] H. Krakauer, M. Posternak, and A. J. Freeman, Phys. Rev. B **19**, 1706 (1979).
[39] H. J. Monkhorst and J. D. Pack, Phys. Rev. B **13**, 5188 (1976).
[40] M. G. Gillan, J. Phys.: Condens. Matter **1**, 689 (1989).
[41] F. D. Murnaghan, Proc. Natl. Acad. Sci. U.S.A. **50**, 697 (1944).
[42] C. Kittel, in *Introduction to Solid State Physics*, 7th ed. (Wiley & Sons, New York, 1996).
[43] A. Khein, D. J. Singh, and C. J. Umrigar, Phys. Rev. B **51**, 4105 (1995).
[44] F. Favot and A. Dal Corso, Phys. Rev. B **60**, 11 427 (1999).
[45] M. Fuchs, M. Bockstedte, E. Pehlke, and M. Scheffle, Phys. Rev.

B **57**, 2134 (1998).
[46] M. Fuchs, J. L. F. Da Silva, C. Stampfl, J. Neugebauer, and M. Scheffler, Phys. Rev. B **65**, 245212 (2002).
[47] V. Fiorentini and M. Methfessel, J. Phys.: Condens. Matter **8**, 6525 (1996).
[48] P. Blaha, K. Schwarz, and J. Luitz, *WIEN97, A Full-Potential Linearized Augmented Plane Wave Package for Calculating Crystal Properties* (Karlheinz Schwarz, Techn. Univ. Wien, Vienna, 1999), ISBN 3-9501031-0-4, Updated version of P. Blaha, K. Schwarz, P. Sorantin, and S. B. Trickey, Comput. Phys. Commun. **59**, 399 (1990).
[49] H. L. Skriver and N. M. Rosengaard, Phys. Rev. B **46**, 7157 (1992).
[50] W. R. Tyson and W. A. Miller, Surf. Sci. **62**, 267 (1977).
[51] C. J. Fall, N. Binggeli, and A. Baldereschi, Phys. Rev. Lett. **88**, 156802 (2002).
[52] J. Furthmüller, G. Kresse, J. Hafner, R. Stumpf, and M. Scheffler, Phys. Rev. Lett. **74**, 5084 (1995).
[53] J. Schöchlin, K. P. Bohnen, and K. M. Ho, Surf. Sci. **324**, 113 (1995).
[54] D. W. Jepsen, P. M. Marcus, and F. Jona, Phys. Rev. B **5**, 3933 (1972).
[55] K.-P. Bohnen and K.-M. Ho, Surf. Sci. **207**, 105 (1988).
[56] H. B. Nielsen, J. N. Andersen, L. Petersen, and D. L. Adams, J. Phys. C **15**, L1113 (1982).
[57] J. N. Andersen, H. B. Nielsen, L. Petersen, and D. L. Adams, J. Phys. C **17**, 173 (1984).
[58] A. Mikkelsen, J. Jiruse, and D. L. Adams, Phys. Rev. B **60**, 7796 (1999).
[59] H. Göbel and P. von Blanckenhagen, Phys. Rev. B **47**, 2378 (1993).
[60] J. R. Noonan and H. L. Davis, Phys. Rev. B **29**, 4349 (1984).
[61] N. Marzani, D. Vanderbilt, A. De Vita, and M. C. Payne, Phys. Rev. Lett. **82**, 3296 (1999).
[62] V. Chis and B. Hellsing, Phys. Rev. Lett. **93**, 226103 (2004).
[63] I. Galanakis, G. Bihlmayer, V. Bellini, N. Papanikolaou, R. Zeller, S. Blügel, and P. H. Dederichs, Europhys. Lett. **58**, 751 (2002).